

The Continuum Emission Spectrum of Hf 2-2 near the Balmer Limit and the ORL versus CEL abundance and temperature Discrepancy

P.J. Storey^{1*}, Taha Sochi^{1*†}

¹University College London, Department of Physics and Astronomy, Gower Street, London, WC1E 6BT

Accepted XXX. Received XXX; in original form XXX

ABSTRACT

The continuum spectrum of the planetary nebula Hf 2-2 close to the Balmer discontinuity is modeled in the context of the long standing problem of the abundance and temperature discrepancy found when analyzing optical recombination lines and collisionally excited forbidden lines in nebulae. Models are constructed using single and double Maxwell-Boltzmann distributions as well as κ -distributions for the energies of the free electrons. New results for the necessary continuum and line emission coefficients are presented calculated with κ -distributed energies. The best fit to the observed continuum spectrum is found to be a model comprising two components with dramatically different temperatures and with a Maxwell-Boltzmann distribution of electron energies. On the basis of a χ^2 analysis, this model is strongly favored over a model with κ -distributed electron energies.

Key words: atomic transition – atomic spectroscopy – Hf 2-2 – planetary nebulae – nebular physics – optical recombination lines – collisionally excited lines – Balmer continuum – abundance discrepancy – electron temperature – electron distribution – Maxwell-Boltzmann – kappa distribution.

Note: figures are colored in the online version.

1 INTRODUCTION

The long standing problem in nebular physics related to the abundance and temperature discrepancy between the results obtained from optical recombination lines (ORL) and collisionally excited lines (CEL) has been visited by many researchers in the last few decades. Several explanations for the general trend of obtaining higher abundances and lower temperatures from ORL than from CEL of the same ions have been put forward. One explanation is a multi-component model of planetary nebulae in which low temperature, high metallicity components (clumps) produce the ORL and are embedded in a high temperature, relatively low metallicity, hydrogen-rich component that produces the CEL (Liu *et al* 2000). It has been suggested recently (Nicholls *et al* 2012) that this discrepancy may be largely explained by the assumption of a different electron energy distribution, a κ -distribution, rather than the Maxwell-Boltzmann (MB) distribution which is tradition-

ally accepted as the dominant distribution in the low density plasma found in the planetary nebulae.

The debate about the electron energy distribution in astronomical objects, including planetary nebulae, is relatively old and dates back to at least the 1940s when Hagi-hara Hagihara (1944) suggested that the distribution of free electrons in gaseous assemblies deviates considerably from the MB distribution. This was refuted by Bohm & Aller (1947) who, on the basis of a detailed quantitative balance analysis, concluded that any deviation from the Maxwellian equilibrium distribution is very small. The essence of their argument is that for typical planetary nebulae conditions, the thermalization process of elastic collisions is by far the most frequent event and typically occurs once every second, while other processes that shift the system from its thermodynamic equilibrium, like inelastic scattering with other ions that leads to metastable excitation or recapture, occur at much larger time scales estimated to be months or even years. Bohm and Aller also indicated the significance of any possible deviation from a Maxwellian distribution on derived elemental abundances. However, nobody seems to have considered non-MB electron distributions as a possible

* E-mail: pjs@star.ucl.ac.uk (PJS).

† E-mail: t.sochi@ucl.ac.uk (TMS). Corresponding author.

solution for the ORL/CEL discrepancy problem until the recent proposal of Nicholls *et al* (2012). In the light of this suggestion, it seems appropriate to ask whether there is any empirical evidence from observation for departures from MB energy distributions in nebulae.

A preliminary investigation of this possibility has been given recently by Sochi (2012) and Storey & Sochi (2013) who proposed a method based on using atomic dielectronic recombination (DR) theoretical data in conjunction with observational line fluxes to sample the free electron distribution and compare to the theoretical distributions, i.e. Maxwell-Boltzmann and κ . For all the objects studied by Storey & Sochi (2013) the limited observational data analyzed were found to be better described by a single MB distribution than a κ -distribution but the uncertainties were sufficient that a κ -distribution could not be conclusively excluded. A two-component model incorporating low temperature material was also found to not fit the data as well as a single MB model.

The current paper approaches this problem by modeling the magnitude of the Balmer discontinuity and nearby Balmer continuum of the planetary nebula Hf 2-2. This nebula is an extreme example of the ORL/CEL discrepancy trend since its abundance discrepancy factor (ADF), defined as the ratio of ORL abundance to CEL abundance, reaches an exceptionally high value between 68-84 (Liu 2003; Wesson *et al* 2003; Zhang *et al* 2004; Liu *et al* 2004; Wesson & Liu 2004; Liu *et al* 2006; Wesson *et al* 2008). An exceptionally high temperature discrepancy between the CEL and ORL results, which differ by about an order of magnitude, has also been obtained for this nebula.

The shape of the Balmer continuum is principally determined by a convolution of the $n = 2$ hydrogen recombination cross-section and the free electron energy distribution. The shape of the continuum therefore offers the possibility of gaining information about the free electron energy distribution. We shall see below that in the case of Hf 2-2 the continuum shape is primarily determined by the free electron energy distribution. In section 2 we outline the properties of Hf 2-2 and in section 3 we deal with the theory describing the continuum processes and new results relating to recombination using a κ -distribution. The fitting procedure and the resulting fits to the spectral data with MB and κ distributions are described in section 4 and our conclusions in section 5.

2 Hf 2-2

Hf 2-2 is a faint southern highly symmetric low density planetary nebula with a central cavity and interior disc-shaped multi-shell structure. Its spectrum includes carbon, nitrogen, oxygen, neon, sulphur and argon lines as well as helium. Hf 2-2 seems to have a high abundance in He and C with a high C/O ratio and an exceptionally strong C II $\lambda 4267$ Å signature. The nebula, which is in the galactic bulge at a distance of about 4.0-4.5 kpc, has a spectrally-varying close binary central system with a period of about 0.40 day (Bond 2000). Hf 2-2 has common spectral features with older novae like DQ Her (Cahn & Kaler 1971; Maciel 1984; Kaler 1988; Liu 2003; Liu *et al* 2006; Schaub *et al* 2012), and therefore being a planetary nebula may be disputed.

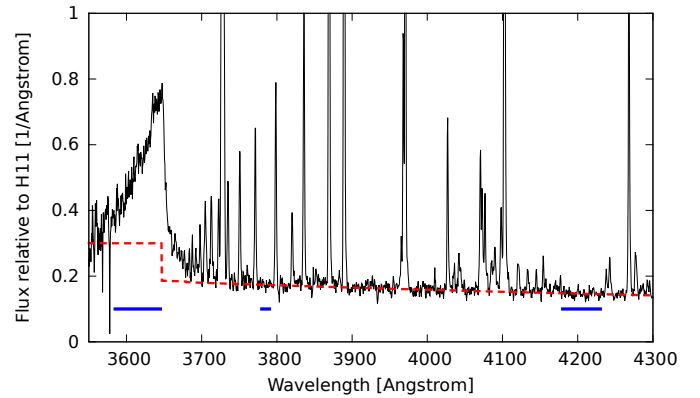


Figure 1. The observed Hf 2-2 spectrum (solid) and the continuum fit with a single Maxwell-Boltzmann distribution with $T = 8800$ K (dashed). The fit was optimized on the two longer wavelength of the three wavelength segments (shown in the figure as horizontal lines): 3585-3645, 3780-3790 and 4180-4230 Å.

This unusual nebula is marked by a number of exceptional features. Hf 2-2 exhibits a very high ADF, possibly the highest recorded for a planetary nebula, with very strong ORL emission. Hf 2-2 also has the very large C/O abundance ratio of about 19 (Patriarchi & Perinotto 1994). A third unusual feature is a very large Balmer jump associated with a rapid fall in the Balmer continuum intensity towards shorter wavelengths. An estimation based on the magnitude of the Balmer discontinuity indicates an electron temperature of about 780-1000 K in sharp contrast to the forbidden lines estimation of about 8800 K from an [O III] line (Liu 2003; Liu *et al* 2004; Zhang *et al* 2004; Liu *et al* 2006; McNabb *et al* 2012). The deduced Balmer discontinuity temperature is one of the lowest observed for a planetary nebula. These findings led Liu *et al* (2006) to conclude that a multi-component model of cold hydrogen-deficient knots embedded into a metal-poor nebula may be inevitable to explain these exceptional observations.

With regard to ORL electron temperature derivations for Hf 2-2, Bastin (2006) obtained a mean electron temperature of < 600 K from C II lines, while Liu (2006) derived an electron temperature of about 630 K and McNabb *et al* (2012) a temperature of about 3160 K from O II lines. As for the stellar temperature of this nebula, it is estimated by Liu *et al* (2006) between 50000–67000 K, while Schaub *et al* (2012) set the temperature of the two stars (assuming a binary system which seems to be largely accepted) in their model to 67000 K and 7500 K.

The observational data of Hf 2-2 which is used in the present paper were obtained in 2001 by a Boller and Chivens long-slit spectrograph mounted on the ground-based 1.52 m European Southern Observatory telescope located in La Silla Chile. More details about this data set can be found in Liu *et al* (2006). The observed spectrum is shown in Figure 1, with the measured flux normalized to Balmer H11, an apparently unblended line close to the Balmer discontinuity.

3 THEORY

To model the magnitude of the Balmer discontinuity and the shape of the Balmer continuum we consider the contributions to the continuum spectrum from recombination of H^+ and He^+ , H 2-photon emission and the underlying scattered stellar continuum. Recombination of He^{2+} is neglected due to the very low He^{2+}/H^+ fraction in Hf 2-2 which is estimated to be about 0.002 (Zhang *et al* 2004; Liu *et al* 2006).

The recombination of an atomic ion X^+ with an electron, e^- of energy E to a state X^* of the recombined ion,

$$X^+ + e^- \rightarrow X^* + h\nu, \quad (1)$$

gives rise to continuous emission with emission coefficient (energy emitted per unit time per unit frequency and per unit particle densities)

$$\gamma^*(\nu) = \frac{h^3 \alpha^3 c}{32\pi^2 m_e a_0^2} \frac{\omega^*}{\omega^+} \left(\frac{h\nu}{R}\right)^3 \left(\frac{R}{E}\right)^{\frac{1}{2}} f(E) \sigma_\nu^* \quad (2)$$

where, ν is the frequency of the emitted photon, ω^+ and ω^* are the statistical weights of the initial and final states respectively, $f(E)$ is the free electron energy distribution function, σ_ν^* is the photoionization cross-section for the inverse process of Equation 1 and R is the Rydberg energy constant. The other symbols have their usual meanings. In the present paper, the photoionization cross-sections for states of H and He are taken from Storey & Hummer (1991) and Hummer & Storey (1998) respectively as described in more detail by Ercolano & Storey (2006).

In this paper we consider two possible forms for $f(E)$, the Maxwell-Boltzmann distribution

$$f_{MB}(E, T) = \frac{2}{(kT)^{3/2}} \sqrt{\frac{E}{\pi}} e^{-\frac{E}{kT}}, \quad (3)$$

where T is the electron temperature, and the κ -distribution (Vasyliunas 1968; Summers & Thorne 1991) given by

$$f_\kappa(E, T_\kappa) = \frac{2\sqrt{E}}{\sqrt{\pi}(kT_\kappa)^{3/2}} \frac{\Gamma(\kappa+1)}{(\kappa-\frac{3}{2})^{\frac{3}{2}} \Gamma(\kappa-\frac{1}{2})} \left(1 + \frac{E}{(\kappa-\frac{3}{2})kT_\kappa}\right)^{-(\kappa+1)} \quad (4)$$

where κ is a parameter defining the distribution, Γ is the gamma-function for the given arguments, and T_κ is a characteristic temperature. Note that f_κ becomes a MB distribution with $T_\kappa \rightarrow T$ as $\kappa \rightarrow \infty$.

The normalization of the continuum flux to H11 flux requires that the effective recombination coefficients for H11 should be calculated both with a Maxwell-Boltzmann distribution and a κ -distribution. The hydrogen line emissivities tabulated by Hummer & Storey (1987) and Storey & Hummer (1991) were calculated assuming that the free electron energy distribution is described by a Maxwell-Boltzmann distribution for all physical processes between bound and continuum states involving free electrons. Here we use the techniques and computer codes described in the last two references and extend them to include a κ -distribution. At the electron number densities typical of photoionized nebulae ($10^2 - 10^5 \text{ cm}^{-3}$) the populations of the low-lying states of H are determined primarily by recombination and radiative cascading and are relatively insensitive to the ambient electron density. Hence any error introduced into the calculation of collision rates between high- n states caused by the use of a Maxwell-Boltzmann distribution rather than a

κ -distribution should have minimal effect at nebular densities. We therefore make the approximation of computing the direct recombination coefficients to all the individual levels using a κ -distribution but retain a Maxwell-Boltzmann distribution for the energy and angular momentum changing collisions among the higher- n states. This should provide a good approximation for the H11 emissivity.

For a general free electron energy distribution, the recombination coefficient to a state X^* is given by

$$\alpha_{RC}^* = \frac{R^{\frac{5}{2}}}{\sqrt{2}c^2 m_e^{\frac{3}{2}}} \frac{\omega^*}{\omega^+} \int_0^\infty \left(\frac{h\nu}{R}\right)^2 \left(\frac{R}{E}\right)^{\frac{1}{2}} \sigma_\nu^* f(E) d\left(\frac{E}{R}\right) \quad (5)$$

On solving the collisional-radiative recombination problem for hydrogen we obtain the recombination coefficients to all levels and the effective recombination coefficients $\alpha_{\text{eff}}(\lambda)$ for a transition of wavelength λ . We define a line emission coefficient $\epsilon(\lambda)$ as the energy emitted per unit volume per unit time for unit ion and electron density, so that

$$\epsilon(\lambda) = \alpha_{\text{eff}}(\lambda) \frac{hc}{\lambda}. \quad (6)$$

Nicholls *et al* (2013) derive the following approximate expression for converting recombination coefficients calculated with a Maxwell-Boltzmann electron energy distribution to those applicable with a κ -distribution,

$$x(\kappa) \equiv \frac{\alpha_\kappa(\lambda)}{\alpha_{MB}(\lambda)} = \frac{\epsilon_\kappa(\lambda)}{\epsilon_{MB}(\lambda)} = \frac{(1 - \frac{3}{2\kappa})\Gamma(\kappa+1)}{(\kappa - \frac{3}{2})^{\frac{3}{2}}\Gamma(\kappa - \frac{1}{2})}. \quad (7)$$

To obtain this result, Nicholls *et al* (2013) use the fact that the photoionization cross-section falls approximately as $(\nu_0/\nu)^3$ for $\nu > \nu_0$, where ν_0 is the threshold frequency for photoionization. so that the integrand in Equation 5 contains a $1/\nu$ term. Nicholls *et al* (2013) simplify the integral by moving the $1/\nu$ term outside of the integral, making it possible to carry out the integration analytically. In practice the integral is a convolution of the free-electron energy distribution with the $1/\nu$ term, which is energy dependent. At low temperatures the rapid fall in the electron energy distribution function with increasing energy means that it is a good approximation to neglect the energy dependence of the frequency term. At higher temperatures, both terms are essential in the calculation of the recombination coefficient. The expression for $x(\kappa)$ in Equation 7 is independent of temperature, density and transition. This approximation will fail at sufficiently high temperatures where the effects of the free-electron energy distribution and the frequency dependent term become comparable.

Using the approximate function $x(\kappa)$, we can express the results of our more complete collisional-radiative treatment for $\epsilon(\lambda)$ in terms of a correction factor $y(\lambda, T, \kappa)$ as follows

$$\epsilon_\kappa(\lambda) = \epsilon_{MB}(\lambda) x(\kappa) y(\lambda, T, \kappa). \quad (8)$$

The values of ϵ_{MB} can be obtained from Hummer & Storey (1987) and Storey & Hummer (1991). In Table 1 we tabulate values of $y(\lambda, T, \kappa)$ for H11 corresponding to various values of κ at a range of temperatures. We also tabulate in the last line x as a function of κ . Note that, in principle, y also depends on electron density but in practice it is very insensitive to electron density for densities up to 10^5 cm^{-3} , so we only tabulate values calculated at 10^3 cm^{-3} .

Table 1. Values of the correction factor $y(\lambda, T, \kappa)$, defined in Equation 8, as a function of κ and $\log T[\text{K}]$ for computing the emission coefficient, $\epsilon_{\kappa}(\lambda)$ for H11. In the last row of the table x , as defined in Equation 7, is given as a function of κ .

$\log T[\text{K}]$	κ						
	50.0	20.0	10.0	7.0	5.0	3.0	2.0
2.6	0.994	0.994	0.996	0.997	0.999	1.004	1.017
2.7	0.994	0.995	0.997	0.999	1.002	1.011	1.031
2.8	0.995	0.996	0.999	1.001	1.005	1.017	1.044
2.9	0.995	0.997	1.001	1.004	1.009	1.024	1.057
3.0	0.996	0.998	1.002	1.007	1.013	1.031	1.071
3.1	0.996	0.999	1.004	1.009	1.016	1.038	1.084
3.2	0.996	1.000	1.005	1.011	1.020	1.045	1.099
3.3	0.996	1.000	1.007	1.013	1.023	1.053	1.115
3.4	0.996	1.000	1.008	1.016	1.027	1.062	1.133
3.5	0.995	1.001	1.010	1.019	1.032	1.072	1.154
3.6	0.995	1.001	1.012	1.022	1.037	1.083	1.177
3.7	0.995	1.001	1.014	1.026	1.043	1.096	1.203
3.8	0.995	1.003	1.017	1.031	1.051	1.112	1.235
3.9	0.995	1.004	1.020	1.036	1.059	1.128	1.269
4.0	0.994	1.004	1.022	1.040	1.066	1.144	1.306
4.1	0.995	1.006	1.027	1.047	1.076	1.165	1.350
4.2	0.995	1.008	1.032	1.054	1.087	1.187	1.398
4.3	0.995	1.010	1.036	1.060	1.097	1.210	1.450
$x(\kappa)$	1.008	1.020	1.043	1.066	1.103	1.228	1.596

As can be seen, the values from Equation 7 are a good approximation for large values of κ but the ratio increases as κ decreases. In addition, the values from Equation 7 are generally smaller than the more exact values, with the difference being largest for the smallest tabulated κ and the highest temperatures, as expected.

Since our model of the recombination process with κ -distributed electron energies does not treat energy and angular momentum changing collisions correctly we cannot use the results to model the high Balmer lines as was done for example by Zhang *et al* (2004) using the code originally authored by one of us (PJS). We therefore restrict the current model to calculation of the continuum processes only, normalized to the H11 flux.

Our model of the continuum also includes the hydrogen 2-photon emission. The emission coefficient for the hydrogen 2s-1s 2-photon emission is

$$\epsilon_{2q}(\nu) = \alpha(2s) \frac{A_{2q}(\nu)}{A_{2q} + C_{2s,2p} N_p} h\nu, \quad (9)$$

where $\alpha(2s)$ is the total recombination coefficient to the 2s state of H, A_{2q} is the total 2s-1s spontaneous transition probability, $A_{2q}(\nu)$ is the probability per unit frequency, $C_{2s,2p}$ is the coefficient for proton collisional transitions between the 2s and 2p states and N_p is the proton number density. We assume that the population of the 2p state is negligible at the relevant densities (Hummer & Storey 1987), and we take $C_{2s,2p}$ from Seaton (1955) and A_{2q} and $A_{2q}(\nu)$ from Nussbaumer & Schmutz (1984). Values of $\alpha(2s)$ for an MB distribution were provided by Hummer & Storey (1987) and Storey & Hummer (1991). From our new calculation of the hydrogen collisional-radiative problem with a κ -distribution we obtain values of $\alpha(2s)$ as a function of κ and temperature. These values can be related to those obtained with an

Table 2. Values of the correction factor $z(2s, T, \kappa)$, defined in Equation 10, as a function of κ and $\log T[\text{K}]$ for computing the total recombination coefficient to the 2s state of hydrogen with κ -distributed electron energies.

$\log T[\text{K}]$	κ						
	50.0	20.0	10.0	7.0	5.0	3.0	2.0
2.6	0.994	0.994	0.995	0.995	0.996	1.000	1.009
2.7	0.994	0.994	0.996	0.997	0.999	1.005	1.020
2.8	0.994	0.995	0.997	0.999	1.001	1.009	1.029
2.9	0.995	0.996	0.998	1.000	1.004	1.014	1.038
3.0	0.995	0.996	0.999	1.002	1.006	1.018	1.047
3.1	0.995	0.996	1.000	1.003	1.007	1.022	1.054
3.2	0.994	0.996	1.000	1.003	1.009	1.025	1.062
3.3	0.994	0.996	1.001	1.004	1.011	1.029	1.070
3.4	0.994	0.996	1.001	1.005	1.013	1.033	1.079
3.5	0.994	0.997	1.002	1.007	1.015	1.038	1.089
3.6	0.994	0.998	1.004	1.009	1.018	1.045	1.101
3.7	0.995	0.999	1.006	1.012	1.022	1.052	1.114
3.8	0.998	1.001	1.010	1.017	1.028	1.062	1.131
3.9	0.997	1.002	1.011	1.019	1.032	1.069	1.147
4.0	0.994	1.000	1.010	1.019	1.033	1.075	1.162
4.1	0.994	1.000	1.011	1.022	1.038	1.085	1.182
4.2	0.995	1.002	1.014	1.026	1.044	1.096	1.207
4.3	0.994	1.001	1.015	1.028	1.048	1.107	1.230

MB distribution in the same way as in Equation 8, via the function $x(\kappa)$

$$\alpha_{\kappa}(2s) = \alpha_{\text{MB}}(2s) x(\kappa) z(2s, T, \kappa) \quad (10)$$

where we tabulate the correction factors $z(2s, T, \kappa)$ in Table 2.

4 MODELING THE CONTINUUM

The observed spectrum of Hf 2-2 with intensity normalized relative to H11 is shown in Figure 1. The figure also shows the spectral segments that we use for fitting, chosen to be as free as possible from significant spectral lines. The wavelength ranges for the three segments are $\lambda = 3585\text{-}3645$, $3780\text{-}3790$ and $4180\text{-}4230 \text{ \AA}$.

4.1 The continuum longward of the Balmer edge

The observed continuum longward of the Balmer edge is comprised principally of hydrogen free-bound emission with principal quantum number $n > 2$, helium free-bound emission, hydrogen 2-photon emission and scattered starlight from the central star of the nebula. The emissivity of the H 2-photon emission relative to H11 is relatively insensitive to the temperature of the emitting material and comprises up to 10% of the continuum in this spectral region. The contribution from $n > 2$ H free-bound emission varies strongly with the temperature, being 3% just longward of the Balmer edge at $T = 10^4 \text{ K}$ and falling rapidly as the temperature decreases. We model the remaining background contribution to the flux relative to H11 with an empirical power-law distribution

$$F(\lambda) = F_0 \left(\frac{3647}{\lambda} \right)^{\beta} \quad (11)$$

Table 3. Underlying continuum fitting parameters F_0 and β for two scenarios (a) A single MB distribution with temperature 8800 K, and (b) a single κ -distribution with $\kappa = 2$ and $T = 3000$ K.

	$F_0 [\text{\AA}^{-1}]$	β
a	0.161	1.588
b	0.174	1.536

where F_0 is the contribution at the Balmer edge and wavelengths in \AA are vacuum wavelengths.

The parameters F_0 and β were obtained by fitting the model continuum to the two longer wavelength segments shown in Figure 1 by minimizing the rms deviations of the fit from the observed spectrum. In computing the model continuum we take $N(\text{He}^+)/N(\text{H}^+) = 0.103$ (Liu *et al* 2006). The same authors quote $N(\text{He}^{2+})/N(\text{H}^+) = 0.002$, which means that He^{2+} recombination makes a negligible contribution to the continuum, so we neglect this component. The derived continuum is very weakly sensitive to the electron number density through the 2-photon component (Equation 9) and we adopt $N_e = 1000 \text{ cm}^{-3}$.

The best fit values of F_0 and β were derived for two models. The first uses a MB distribution for the free electrons with a temperature of 8800 K chosen to reflect the forbidden line values derived by Liu *et al* (2006). In any model comprising two MB distributions, the low temperature component will contribute a negligible amount to the continuum longward of the Balmer edge, so it is appropriate to use the forbidden line temperature to determine the continuum component in this wavelength range.

As we shall see below, the best fit to the continuum using a single κ -distribution yields an electron temperature of a few thousand Kelvin and a small value of κ . So for our second model of the underlying continuum we adopt a κ -distribution with $\kappa = 2$ and $T = 3000$ K. The results of the two underlying continuum models are summarized in Table 3. The values of F_0 and β are relatively insensitive to the assumptions about the electron energy distribution and its temperature. To illustrate the fit longward of the Balmer edge, we show in Figure 1 the full fit to the two longer wavelength segments of the continuum including all the processes described above, using the parameters (a) from Table 3 and assuming a single MB distribution with $T = 8800$ K.

4.2 Fits with Maxwell-Boltzmann distributions

It is clear from Figure 1 that the magnitude of the Balmer discontinuity and the slope of the Balmer continuum shortward of the discontinuity cannot be explained by emission from hydrogen and helium at the forbidden line temperature. This has already been discussed by Liu *et al* (2006) who estimated that the shape of the continuum implies that the emitting region has a temperature of ≈ 900 K. In Figure 2 we show the result of making a fit to all three spectral segments shown in Figure 1 using a single MB electron energy distribution in which the temperature is a free parameter. The background continuum is computed using the

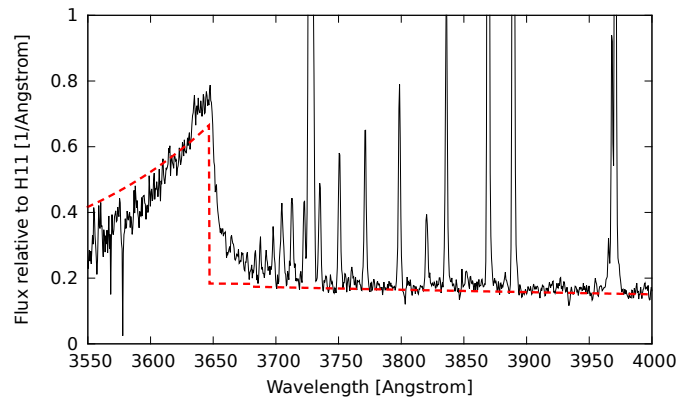


Figure 2. The observed Hf 2-2 spectrum (solid) and the single-component Maxwell-Boltzmann fit (dashed) where the temperature is treated as a free parameter. The final optimized temperature is $T = 1334$ K.

parameters from fit (a) in Table 3. The temperature of best fit is 1334 K and although the continuum model is improved compared to Figure 1, it matches neither the magnitude of the discontinuity nor the slope adequately.

As discussed earlier, one resolution of the ORL/CEL abundance and temperature discrepancy in nebulae that has been proposed is that there are relatively cold high-metallicity knots embedded in hotter lower abundance gas. We therefore attempt to match the continuum with two components having different temperatures. We set the temperature of one component equal to a typical forbidden line temperature for this object of 8800 K and allow the other to vary. The continuum emissivity has only weak density dependence so we choose representative electron densities for the two components of 1000 cm^{-3} for the forbidden line region and 5000 cm^{-3} for the cold material (Liu *et al* 2006). The relative emission measure of the two components is then allowed to vary by making the volume ratio of the two components a free parameter. In Figure 3 we show the resulting fit, which is excellent. The optimum temperature of the cold component is 540 K and the fraction of the total volume occupied by the cold component is 0.00706. Hence the cold component has an emission measure, which is proportional to the product of the volume fraction and particle density squared, that is 15.0% of the total recombination line and continuum emission measure.

4.3 Fit with κ -distribution

An alternative possible resolution of the ORL/CEL problem is that there is no separation of the emitting material into high and low temperature components with significantly different abundances but rather a single medium in which the electron energy distribution is non-Maxwellian, with a κ -distribution being a possible candidate. The Balmer continuum close to the Balmer discontinuity provides a means of testing the validity of this proposal for the very low energy part of the distribution function. In Figures 4 and 5 we illustrate how the magnitude of the Balmer discontinuity and shape of the Balmer continuum change as κ is varied for two different temperatures. Compared to a MB, κ -distributions have more particles at the lowest and highest

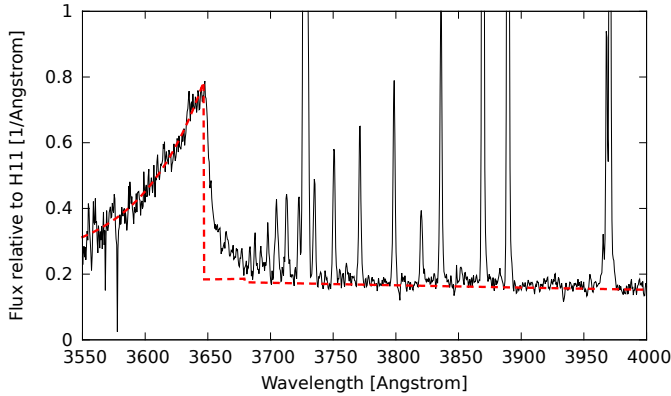


Figure 3. The observed Hf 2-2 spectrum (solid) and a two-component Maxwell-Boltzmann fit (dashed) with two temperatures: one is the forbidden line temperature which is fixed at $T = 8800$ K and the other is free to vary. The ratio of the volumes of the two components is also treated as a free parameter.

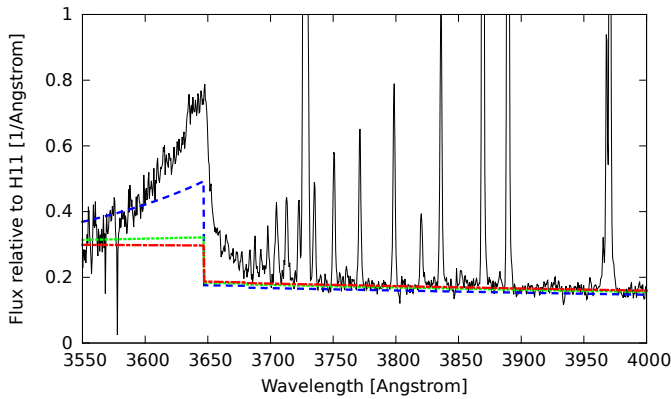


Figure 4. Model continua with a κ -distribution of electron energies for a temperature $T = 10000$ K; $\kappa = 2$ (dashed blue line), $\kappa = 5$ (dotted green line), and $\kappa = 25$ (dot-dashed red line).

energies and less at intermediate energies. At low energies the κ -distribution function thus falls more rapidly with increasing energy than a MB distribution. This can be seen in Figure 5, for example, with the magnitude of the Balmer discontinuity increasing and the slope of the Balmer continuum becoming steeper as κ decreases.

We now fit the chosen three spectral segments to a κ -distribution of which the temperature and value of κ are free parameters and the final values that we obtained for these parameters are $\kappa = 2.11$ and $T = 4640$ K. Figure 6 shows a plot of this fit. On visual inspection the best-fit κ distribution where κ and temperature are allowed to vary is significantly less good than the two-component MB fit. It should be remarked that the optimized κ obtained from this fitting exercise is very different to values proposed by Nicholls *et al* (2012) which usually fall in the range 10-20. For comparison, we include in Figure 6 a fit carried out with a fixed value of $\kappa = 10$. The temperature was allowed to vary and the best fit value was 1665 K. In the next section we attempt to quantify the relative quality of these fits.

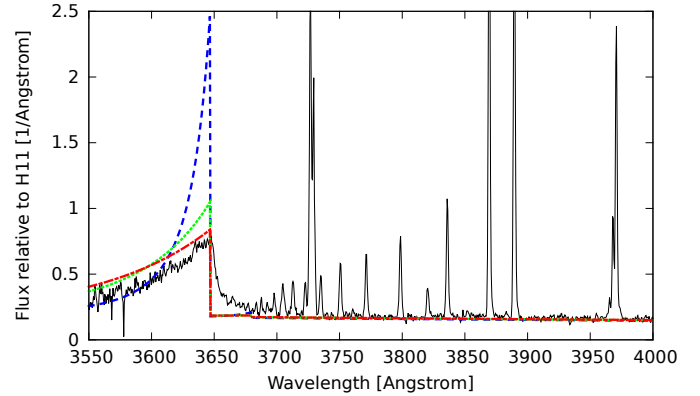


Figure 5. Model continua with a κ -distribution of electron energies for a temperature $T = 1000$ K; $\kappa = 2$ (dashed blue line), $\kappa = 5$ (dotted green line), and $\kappa = 25$ (dot-dashed red line).

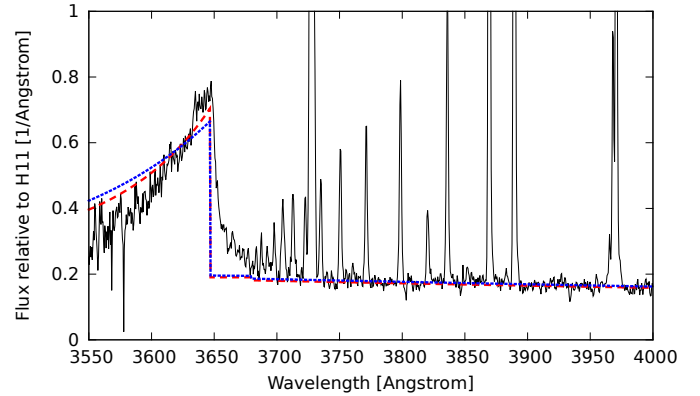


Figure 6. Fits obtained by simultaneous optimization of κ and T (dashed red line) and by fixing $\kappa = 10$ and allowing T to vary (dotted blue line).

4.4 Statistical Analysis

We wish to address the question of whether the fit to the continuum using a κ -distribution is significantly worse than the two-component MB fit. A visual inspection of Figures 3 and 6 shows that while the two-component fit provides a very good match to the three segments of the continuum used for fitting, the best κ -distribution fit underestimates the magnitude of the Balmer discontinuity and also underestimates the steepness of the decline at shorter wavelengths. We will use a comparison of χ^2 values for these two fits to quantify the relative goodness of fit. To estimate χ^2 we need an estimate of the uncertainties on the observational data, which by inspection and from instrumental considerations are not independent of wavelength, being much larger at the shortest wavelengths. We therefore compute separate rms deviations of the data from the two-component MB fit for each of the three wavelength segments. Since we use deviations from the two-component fit to define the data uncertainties it follows that the value of χ^2 for the fit, summed over the three wavelength segments, will be given by

$$\chi^2 = N_{df} \equiv N_{dp} - N_{fp} = 237, \quad (12)$$

where N_{df} is the number of degrees of freedom, N_{dp} is the number of data points in the three segments and N_{fp} is the number of free parameters. We now use the estimates of the data uncertainties from the two-component MB fit to compute χ^2 for the best fit κ -distribution and we find $\chi^2 = 433$. We wish to test the null hypothesis that the κ -distribution is an equally good fit to the data as the two-component MB fit. The following square-root transformation of χ^2 (Abramowitz & Stegun 1972),

$$t = \sqrt{2\chi^2} - \sqrt{2N_{df}}, \quad (13)$$

is such that for large N_{df} , the transformed distribution is approximately normal with zero mean and unit standard deviation. For the best fit κ -distribution we find that $t = 7.67$ standard deviations from the zero mean, indicating that the probability that the null hypothesis is true is vanishingly small.

Thus, a two-component Maxwell-Boltzmann model is highly favored compared to the single-component κ model. The single-component MB model is even less likely to be correct than either of the two-parameter models based on the same χ^2 analysis, giving $t = 14.4$ standard deviations.

5 CONCLUSIONS

The analysis of the Balmer continuum spectrum of Hf 2-2 seems to indicate the signature of a two-component nebula with two different temperatures. Assuming that one component has a temperature of 8800 K, we find that the best fit to the data is obtained by adding a second component with temperature of 540 K and emission measure 15.0% of the total. We also modeled the continuum with a single component with κ -distributed free electron energies, but on the basis of a χ^2 test we found this model to be significantly less likely to be correct. In the case of κ -distribution models, it is important to note that modeling the Balmer continuum only samples the free electron energy distribution at the lowest energies, below the mean energy, and therefore gives no information about departures from MB at energies above the mean energy which might affect the excitation of nebular forbidden lines, for example. The extreme nature of Hf 2-2 and the similarity of some of its spectral features to old novae like DQ Her may also cast some doubt on the applicability of the conclusions reached to the properties of planetary nebulae in general.

6 ACKNOWLEDGMENT AND STATEMENT

The work of PJS was supported in part by STFC (grant ST/J000892/1). During the final stages of writing this paper, our attention was drawn to a similar paper by Y. Zhang, X-W. Liu and B. Zhang (arXiv:1311.4974); however this did not have an impact on the methods or results reported in the present paper.

REFERENCES

- Abramowitz M., Stegun I.A. (eds.), 1972, Handbook of Mathematical Functions with Formulas, Graphs, and Mathematical Tables, Dover Publications New York, ISBN 978-0-486-61272-0, p941 7
- Bastin R., 2006, PhD thesis, University College London 2
- Bohm D., Aller L.H., 1947, ApJ, 105, 131 1
- Bond H.E., 2000, in: Asymmetrical Planetary Nebulae II: From Origins to Microstructures, 199, 115 2
- Cahn J.H., Kaler J.B., 1971, ApJS, 22, 319 2
- Ercolano, B., Storey, P.J., 2006, MNRAS 372, 1875 3
- Hagihara Y., 1944, Proceedings of the Japan Academy, 20, 493 1
- Hummer D.G., Storey, P.J., 1987, MNRAS 224, 801 3, 4
- Hummer D.G., Storey, P.J., 1998, MNRAS 297, 1073 3
- Kaler J.B., 1988, Astronomical Society of the Pacific, 100, 620 2
- Liu X.-W., Storey P.J., Barlow M.J., Danziger I.J., Cohen M., Bryce M., 2000, MNRAS, 312, 585 1
- Liu X.-W., 2003, In: Planetary Nebulae: Their Evolution and Role in the Universe, 209, 339 2
- Liu X-W., 2006, International Astronomical Union (Symposium S234), 2, 219 2
- Liu X.-W., Barlow M.J., Zhang Y., Bastin R.J., Storey P.J., 2006, MNRAS, 368, 1959 2, 3, 5
- Liu Y., Liu X.-W., Barlow M.J., Luo S.-G., 2004, MNRAS, 353, 1251 2
- Maciel W.J., 1984, A&AS, 55, 253 2
- McNabb I.A., Fang X., Liu X.-W., Bastin R., Storey P.J., 2012, Proceedings of the International Astronomical Union (Symposium S283), 7, 432 2
- Nicholls D.C., Dopita M.A., Sutherland R.S., 2012, ApJ, 752, 148 1, 2, 6
- Nicholls D.C., Dopita M.A., Sutherland R.S., Kewley L.J., Palay E., 2013, ApJS, 207, 1 3
- Nussbaumer, H., Schmutz, W., 1984, A&A, 138, 495 4
- Patriarchi P., Perinotto M., 1994, A&A, 287, 585 2
- Schaub S.C., Bodman, E.H.L., Hillwig T.C., 2012, South-eastern Association for Research in Astronomy, 5, 2 2
- Seaton, M.J., 1955, Proc. Phys. Soc. A, 68, 457 4
- Sochi T., 2012, PhD thesis, University College London 2
- Storey, P.J., Hummer, D.G., 1991, CoPhc 66, 129 3
- Storey, P.J., Hummer, D.G., 1995, MNRAS 272, 41 3, 4
- Storey P.J., Sochi T., 2013, MNRAS, 430, 599 2
- Summers D., Thorne R.M. 1991, Phys. Fluids B, 3, 1835 3
- Vasyliunas V.M., 1968, JGR, 73, 2839 3
- Wesson R., Liu X.-W., Barlow M.J., 2003, MNRAS, 340, 253 2
- Wesson R., Liu X.-W., 2004, MNRAS, 351, 1026 2
- Wesson R., Barlow M.J., Liu X.-W., Storey P.J., Ercolano B., De Marco O., 2008, MNRAS, 383, 1639 2
- Zhang Y., Liu X.-W., Wesson R., Storey P.J., Liu Y., Danziger I.J., 2004, MNRAS, 351, 935 2, 3, 4